ADVANCES IN ATMOSPHERIC SCIENCES, VOL. 21, NO. 6, 2004, 868–878

Effect of the Lower Boundary Position of the Fourier Equation on the Soil Energy Balance

SUN Shufen* (孙菽芬) and ZHANG Xia (张 霞)

State Key Laboratory of Numerical Modeling for Atmospherics Sciences and Geophysical Fluid Dynamics, Institute of Atmospheric Physics, Chinese Academy of Sciences, Beijing 100029

(Received 26 February 2003; revised 14 April 2004)

ABSTRACT

In this study, the effect of the lower boundary position selection for the Fourier equation on heat transfer and energy balance in soil is evaluated. A detailed numerical study shows that the proper position of the lower boundary is critical when solving the Fourier equation by using zero heat flux as the lower boundary condition. Since the position defines the capacity of soil as a heat sink or source, which absorbs and stores radiation energy from the sky in summer and then releases the energy to the atmosphere in winter, and regulates the deep soil temperature distribution, the depth of the position greatly influences the heat balance within the soil as well as the interaction between the soil and the atmosphere. Based on physical reasoning and the results of numerical simulation, the proper depth of the position should be equal to approximately 3 times of the annual heat wave damping depth. For most soils, the proper lower boundary depth for the Fourier equation should be around 8 m to 15 m, depending on soil texture.

Key words: thermal conductivity, lower boundary position, effect on heat balance

1. Introduction

The interactive physical processes between different land surface covers and the climate system have been studied for a long time. Due to limitations of observed data and knowledge available about the land surface process now, many land surface models (LSMs) developed since the 1980s have no alternative but to include many parameterization schemes and parameters with much uncertainty. So, a good understanding of the effects from the uncertainty of the schemes and parameters has been a major subject of the important international efforts such as PILPS and GEWEX. Many sensitivity studies have sought to discuss the effect from different scheme designs and parameter selections in the LSMs.

Atmosphere circulation will be strongly dependent on the energy flux partition on the ground surface as well as on the soil temperature profile. Variations or anomalies in either soil surface temperature or deep soil temperature will significantly impact the atmospheric process. Wang (1991) indicated that an anomaly of 1°C in the ground surface temperature over 30 days would cause significant increases in precipitation, air temperature, and humidity as well as a decrease in surface level pressure. Tang and Reiter (1986) found that deep soil temperature over the United States has an impact on precipitation anomalies of the subsequent season. Retnakumari et al. (2000) showed that pre-monsoon soil temperature affects monsoon rainfall at a tropical meteorological station. Xue (2002) demonstrated that deep soil temperature over the western US in late spring has an impact on the summer U.S. precipitation, which could have a substantial implication for the North American snow-monsoon interactions. Thus, Gonzalez-Rouco at al. (2003) suggested that ground temperature, especially deep soil temperature, is a good proxy for annual surface air temperature.

Basically, the spatial distribution and temporal variation of soil temperature are regulated by ground surface heat fluxes and can be described by the thermal transport equation-Fourier equation. However, before the late 1980s, due to the limitation of computer resources, the prediction of soil temperature in most LSMs was performed by a simple but not very accurate scheme, the Force Restore method (Deardorff, 1978; Lin, 1980). Afterwards, the rapid development

*E-mail: ssf@lasg.iap.ac.cn

of computers provided a powerful tool to apply more sophisticated schemes to the LSMs. One important step in LSM development was to solve the Fourier equation (Bonnan, 1996) explicitly instead of using its simplified version, the Force-Restore method. At the same time, a critical issue of how to determine the lower boundary condition for the equation solution was raised naturally. The existing LSMs using the Fourier equation have paid much attention to the surface layer thickness determination because developers of the models are clearly aware of the important influence of the layer thickness on the surface temperature and in turn on the surface energy balance. For the lower boundary condition of the Fourier equation, a zero heat flux was used in most LSMs because of the difficulty in determining an accurate heat flux in the soil bottom layer. The selection of the lower boundary position with the zero flux condition, however, seems to vary widely and be quite arbitrary. For example, a value at 1 m was used by Avissar and Piekle (1989), 1.158 m–3.49 m by Dai and Zeng (1997); 4.25 m by Thompson and Pollard (1995); 4.1 m by Verseghy (1991); 2.89 m by Viterbo and Beljaars (1995); 6.3 m by Bonan (1996), and a value of more than 6.0 m by Roesch at al. (1997) who mentioned the importance of the lower boundary position setting. One exception is Linch-Stieglitz (Lynch-Stieglitz, 1994), who used a non zero heat flux condition at a depth of 2.3 m in the GISS (Goddard Institute for Space Studies) model earlier (1994) and used a zero heat flux condition but emphasized the placement of the lower boundary position at a depth of 10 m later (2001). Thus, we ask whether a correct lower boundary position with the zero flux condition for the Fourier equation is important for energy partition and temperature profile prediction. If the answer is positive, we ask further where the right boundary position is. The goal of this paper is to elucidate the above questions through physical reasoning and a model simulation.

In this paper, the soil model is described in section 2, the correct estimation of the lower boundary position is illustrated in section 3, the result of the numerical experiment is analyzed in section 4, and a conclusion and discussion are given in section 5.

2. Description of the soil model

The study of heat and water transport within soil is based on the coupled moisture and heat transport model (CMHM) (Philip and Devries, 1975; Rosema, 1975; Sun, 1987; Milly, 1982; Scanlon and Milly, 1994). Based on CMHM, Sun et al. (2003) derived a simplified version of the model without loss of accuracy. The basic equations for soil moisture and temperature distribution from the simplified version are given by:

$$\frac{\partial\theta}{\partial t} = \frac{\partial}{\partial z}\left[(D_{\theta\mathrm{L}} + D_{\theta\mathrm{V}})\frac{\partial\theta}{\partial z}\right] + \frac{\partial}{\partial z}\left(D_{\mathrm{TV}}\frac{\partial T}{\partial z}\right) - \frac{\partial K}{\partial z} \tag{1}$$

$$C\frac{\partial T}{\partial t} = \frac{\partial}{\partial z}\left(k\frac{\partial T}{\partial z}\right) \tag{2}$$

where t and z are the time and depth, $\theta(z)$ and $T(z)$ are soil volumetric water content and temperature, C is soil volumetric heat capacity, k is soil thermal conductivity, K and $D_{\theta\mathrm{L}}$ (Clapp and Hornberger, 1978) are liquid moisture hydraulic conductivity and diffusivity of soil, and $D_{\theta\mathrm{V}}$ and D_{TV} (Sun et al., 2003) represent the diffusivities contributed by vapor movement due to moisture content gradient and temperature gradient in the soil.

Equations (1) and (2) are solved by using the implicit finite difference scheme and the Newton-Raphson iterative method. The time step is 15 minutes, and the spatial interval varies from the surface to the bottom, increasing exponentially downwards. Near the soil surface where the variable gradients are normally very sharp, a small interval should be used and the surface layer thickness should be less than 2 cm. In order to simulate the temperature distribution around the surface accurately, there should be several sub-layers located within the damping depth of the diurnal temperature wave. Within a depth of 1.5 m, the model uses about 20 soil layers. When the lower boundary position is lower than 1.5 m, the number of soil layers should increase. The relatively fine vertical structure of the soil model can improve the accuracy of the model simulation results.

3. Estimation of the lower boundary position with the zero flux condition

Equations (1) and (2) need upper and lower boundary conditions. They are:

$$-(D_{\theta\mathrm{V}} + D_{\theta\mathrm{L}})\frac{\partial\theta}{\partial z} - D_{\mathrm{TV}}\frac{\partial T}{\partial z} + K = -E/\rho_{\mathrm{w}} + I \tag{3}$$

$$\frac{\partial\theta}{\partial z} = 0 \tag{4}$$

$$-K_{\mathrm{s}}\frac{\partial T}{\partial z} = R_{\mathrm{n}} - H_{\mathrm{s}} - LE \tag{5}$$

$$\frac{\partial T}{\partial z} = 0 \text{ (Corresponding to zero heat flux at the bottom)} \tag{6}$$

Equations (3) and (4) are the upper and the lower boundary conditions, respectively, for Eq. (1). Equations (5) and (6) are the upper and the lower boundary conditions, respectively, for Eq. (2). ρ_w is water density, R_n, LE, and H_s are net radiation, latent heat, and sensible heat on the soil surface, and I is the infiltration rate.

Table 1. The heat capacify and thermal conductivity calealated from J75 for six exemplifical soils.

θ	k (W m^{-1} K^{-1})	C (J m^{-3} K^{-1})
Clay		
0.05	0.202	1299000
0.10	0.538	1509000
0.20	0.874	1929000
0.30	1.071	2349000
0.40	1.210	2769000
0.48	1.300	3113400
Silt loam		
0.05	0.197	1481000
0.10	0.532	1691000
0.20	0.867	2111000
0.30	1.062	2531000
0.40	1.201	2951000
0.485	1.294	3308000
Loam		
0.05	0.264	1422000
0.10	0.662	1632000
0.20	1.060	2052000
0.30	1.292	2472000
0.40	1.458	2892000
0.451	1.527	3106200
Sandy clay		
0.05	0.327	1385000
0.10	0.789	1595000
0.20	1.250	2015000
0.30	1.519	2435000
0.40	1.710	2855000
0.426	1.752	2964200
Sandy loam		
0.05	0.313	1530000
0.10	0.799	1740000
0.20	1.285	2160000
0.30	1.569	2580000
0.40	1.771	3000000
0.435	1.830	3147000
Sand		
0.05	0.486	1673000
0.10	1.188	1883000
0.20	1.890	2303000
0.30	2.301	2723000
0.35	2.457	2933000
0.395	2.580	3122000

The main problem is determining the proper lower boundary position for Eq. (6). From a strict mathematical point of view, the correct position should be infinitely deep in order to completely include the entire heat capacity of the soil body to absorb or release heat energy. In practical and computational applications, however, the position can only be fixed at a proper specified depth. At the same time, it is required that the temperature gradient or the heat flux must be insured to approach zero at the specified depth, otherwise it may cause some artificial energy added into or extracted from the model simulation, which would, to some degree, distort the soil temperature solution. However, by inspecting existing LSMs, you will find a random selection of the position ranging from 1 m to 6 m as mentioned in section 1 .

The right position is related to the damping depth of the annual heat wave defined in the Force-restore method. Even though the Force-restore method is an approximation of the Fourier Eqs. (2) and (6), its solution correctly reveals the propagation of two different temperature waves characterized with different damping depths in the soil. One is the diurnal temperature wave whose amplitude decreases exponentially, $\sim \exp(-z/d)$, in a shallow surface layer with damping depth $d(O\ (10\ \text{cm}))$(O represents the order of magnitude). The wave propagation is important because it mainly dominates the diurnal variation of surface temperature. The other is the annual (or seasonal) temperature wave whose amplitude also decreases exponentially, $\sim \exp(-z/D)$, in the deep soil layer with damping depth $D(O\ (1\text{–}5\ \text{m}))$. This wave is also very important because the propagation and attenuation of the wave basically defines the seasonal temperature distribution and variation in the entire deep soil zone, which in turn determines the full capacity for the soil body to store the heat energy and regulate the amount of heat energy absorbed in the warm season and released in the cold season. Deardorff (1978) and Lin (1980) proved that the annual waves of temperature T and ground heat flux G both propagate vertically according to $T = T_0 + \Delta T e^{-z/D}\sin(\tilde{\omega}t)$ and $G = (k/D)\Delta T e^{-z/D}\sin(\omega t) = \Delta G e^{-z/D}\sin(\tilde{\omega}t)$ where $D = \sqrt{365}d$ ($d = \sqrt{86400k/(\pi C)}$). This means that, if the variation amplitude of annual temperature or ground heat flux at the ground surface is O (ΔT or ΔG) $\approx O$ (20° to 30°C or 50 W m^{-2}), the variation amplitude of annual temperature or ground heat flux is $O(e^{-1}\Delta T$ or $\Delta G) \approx O(0.37\Delta T \approx 7.4$ to 11°C or 19 W m^{-2}) at depth $D, O(e^{-2}\Delta T$ or $\Delta G) \approx O(0.135\Delta T \approx 2.7$ to 4.0°C or 6.8 W m^{-2}) at depth 2 D, and $O(e^{-3}\Delta T$ or $\Delta T) \approx O(0.05\Delta T \approx 1.0$ to 1.5°C

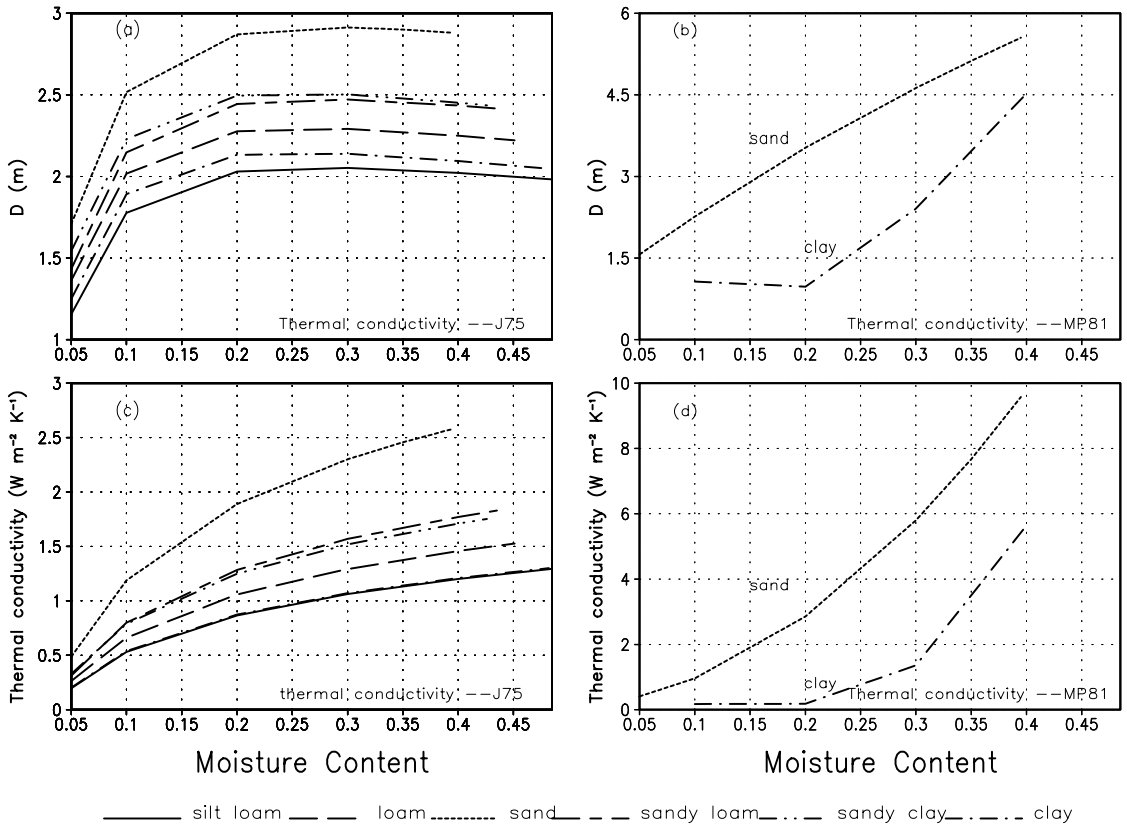

Fig. 1. Variation of damping depth of annual temperature wave (a), (b) and the thermal conductivity (c), (d) with the moisture content for different soil textures.

or 2.5 W m^{-2}) at depth $3D$. This indicates that the heat flux and temperature variation in the soil will not be reduced to a very small value or to zero at a depth less than $2D$. This clearly tells us the right lower boundary position should be located around depth $3D$ from the ground surface if a zero flux is used as the lower boundary condition for the Fourier equation.

The damping depth $D=\sqrt{365}d(d=\sqrt{86400k/(\pi C)}$ is closely related to the soil thermal heat capacity and conductivity. The heat capacity C (J K^{-1} m^{-3}) is estimated by Peters-Lidard et al. (1998) as

$$C = (1942\theta_{\rm m} + 2503\theta_{\rm o} + 4186\theta)10^3\,, \qquad (7)$$

where $\theta_{\rm m}$ is the volumetric content of minerals, $\theta_{\rm o}$ the volumetric content of organic minerals, and θ the volumetric moisture content in the soil. For the thermal conductivity, there are several empirical schemes that are used very often, such as scheme J75 (Peters-Lidard et al, 1998) and scheme MP81+CH78 (later called MP81) (McCumber and Pielke, 1981), which show great discrepancies between them, especially in a wet soil case. Table 1 gives the results of the heat capacity and thermal conductivity calculated from J75 for six exemplified soils: clay, silt loam, loam, sandy clay, sandy loam, and sand, based on the formula and data used by Peters-Lidard et al. (1998). It can be found from Table 1 that, for each soil, the heat capacity for wet soil is around 2.0 times as large as that for dry soil, and the conductivity for wet soil is around six times or more as large as that for dry soil. This indicates that the change of thermal conductivity with moisture content has a more decisive influence on the damping depth of the annual temperature wave. Figures 1c and 1d display the disparities of the thermal conductivities from the schemes of J75 and MP81. The conductivity magnitude from MP81 can be five times larger than that from J75 for wet soil. Figure 1a presents the damping depths of the annual temperature wave for the six soil textures based on J75, and Fig. 1b for clay and sand based on MP81. In the Fig. 1a, the damping depth D from J75 for the six soil textures changes from 1.2 m–1.7 m under dry conditions to 1.7 m–2.8 m under wet conditions, and in Fig. 1b, the damping depth D from MP81 changes from 1.0 m–1.5 m under dry conditions to 4.5 m–5.5 m under wet conditions. In order to cover the whole range of soil moisture and soil texture and to take different conductivity schemes into consideration, the entire

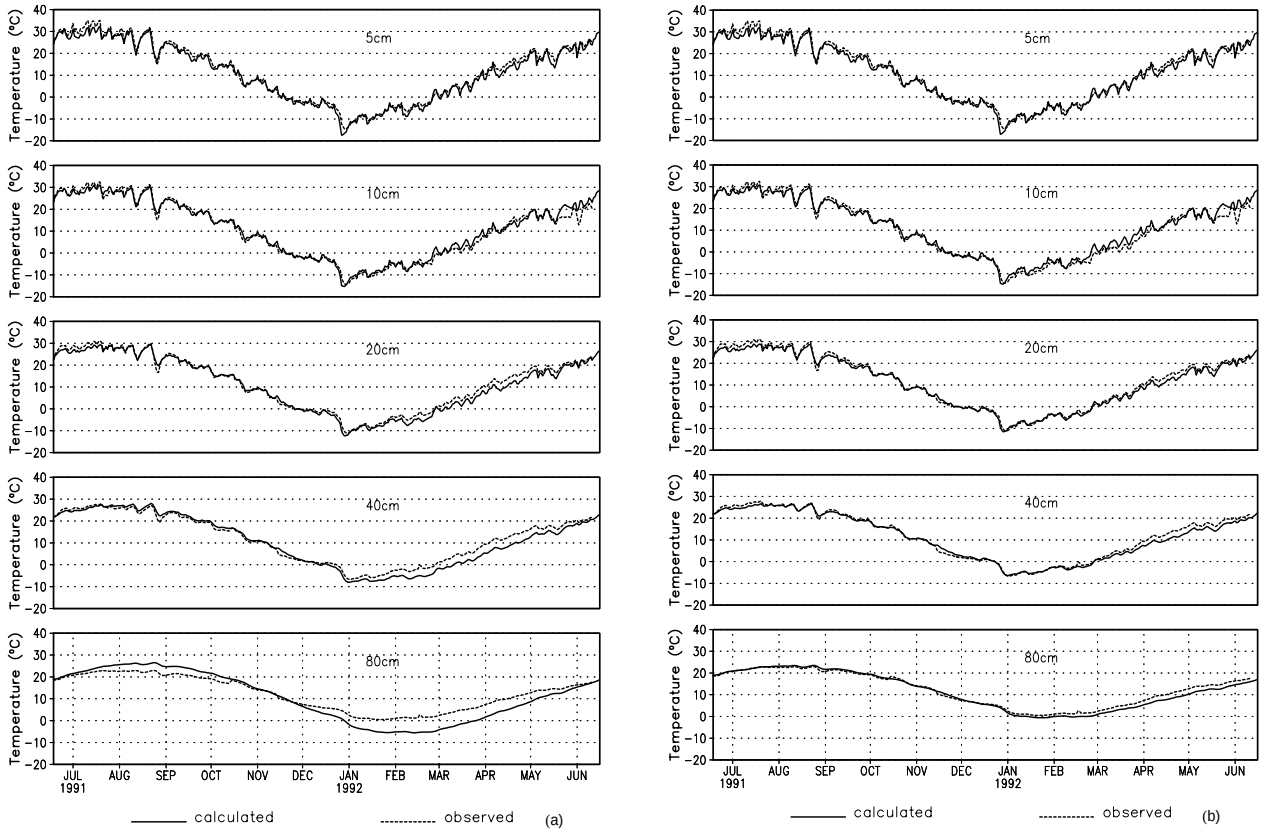

Fig. 2. Daily mean soil temperature at the indicated depths with the lower boundary position 1.5 m deep (a), 3 m deep (b), 6 m deep (c), 10 m deep (d) for HEIFE desert station.

range covers 1 m–5.5 m, and a reasonable upper limit of the maximum D should be from 2.8 m to 5.5 m. According to the reasoning given above, the lower boundary position with zero flux should be located at a depth around $3D$ (8 m–15 m) (the accurate estimation depends on soil texture and soil moisture).

4. Results of numerical experiments

In order to verify the inference in section 3, the effect of the bottom position with different depths on the temperature profile and heat transfers is examined by simulating observed field data from the HEIFE (Heihe river basin Field Experiments) experiment. The data for one year is from a desert station of the HEIFE experiment plan conducted in the Heihe region in western China, where the soil texture is sand and the soil moisture is in a very dry situation because the annual rainfall is around 60 mm and the total potential evaporation is around 2000 mm. An empirical scheme (later called NIU) of thermal conductivity k for sand being used in this study is obtained from the Heihe field observation data in China (Gao and Hu, 1994; Niu, 1995) and is expressed as

$$k = 0.8 + 1.4\theta - (0.8 - 0.3)\exp(-27.0\theta^4)\ .$$

The thermal conductivity from NIU is close to that from J75 in the dry case. But it is only half of the conductivity from J75 and around one tenth of the conductivity from MP81 in the wet case.

The effects of the lower boundary position on temperature distribution are numerically investigated. Figure 2 shows the comparison of the predicted daily mean soil temperatures with observations above the depth of 80 cm at the Heihe desert station for different lower boundary positions (with depths of 1.5 m, 3 m, 6 m, and 10 m). From the figure, one can find that the predicted temperatures around the surface layer within a depth of 20 cm are not affected by shifting the boundary position, and all are very close to each other and are in good agreement with the observations (refer to the curves at depths of 5 cm, 10 cm, and 20 cm). This is because variations of the temperatures near the surface layer within the diurnal heat wave penetration depth are mainly controlled by the diurnal heat-forcing wave and are little influenced by the annual heat-forcing wave. However, for the region

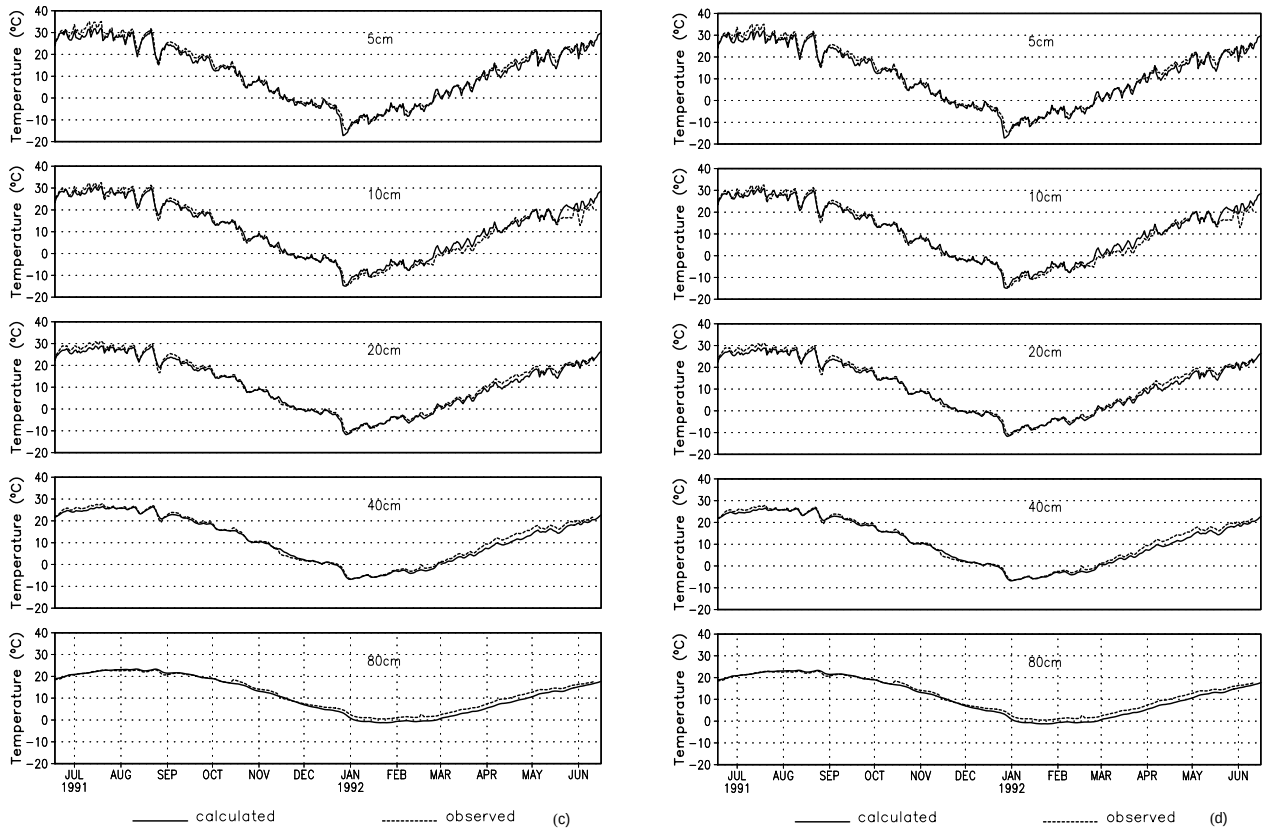

Fig. 2. (Continued)

deeper than 40 cm, the temperatures predicted with different boundary positions are somehow different from each other, and the predicted temperatures with the deeper boundary position show agreement with the observations better than those with a shallower boundary position. This is because the soil temperature at a depth below $O(2d)$ begins to be affected by different boundary position settings.

In order to show the effect of the lower boundary position on temperature distribution further into the deeper soil zone, two numerical tests at the Heife desert station are conducted with different moisture conditions but with same air forcing condition and sand soil property: one is in dry conditions with real measured initial moistures, and one is in wet conditions with a constant moisture during the model simulation period.

For the dry case, k (W m^{-1} K^{-1}) from NIU is equal to about 0.33 (W m^{-1} K^{-1}) and the corresponding D is around 1.46 m. Figure 3 displays the comparison of daily average temperature distributions at the deeper depths of 1.5 m, 3 m, and 6 m in the soil by using different lower boundary depths of 1.5 m (long and short dashed line), 3 m (dotted line), 6 m (dashed line) and 10 m (solid line). For the temperatures at a depth of 1.5 m shown in Fig. 3a, there is a great discrepancy of 10°C between the temperature with the boundary position 1.5 m and the temperatures with the other boundary positions (3 m, 6 m, or 10 m). There is only a small variation among the temperatures with the boundary positions of 3 m, 6 m, and 10 m (equal to or less than 2°C). The range of the annual temperature wave at a depth of 1.5 m with the boundary position 1.5 m deep varies from –5°C to 25°C approximately, but the range of the annual temperature wave at the same depth with other boundary positions (3 m, 6 m, or 10 m) are close to each other and change only from 4°C to 12°C approximately. For the temperatures at a depth of 3 m in Fig. 3b, there is a moderate variation of 5°C between the temperature with the boundary position 3 m deep and that with boundary positions 6 m or 10 m deep, and there is a very small difference between the temperatures with the boundary positions 6 m and 10 m. The amplitude of the annual temperature wave at a depth of 3 m with the boundary position 3 m deep reaches approximately 8°C, but the amplitudes of the annual temperature wave with other boundary depths (6 m and 10 m) decrease to about 2°C. Then, by view-

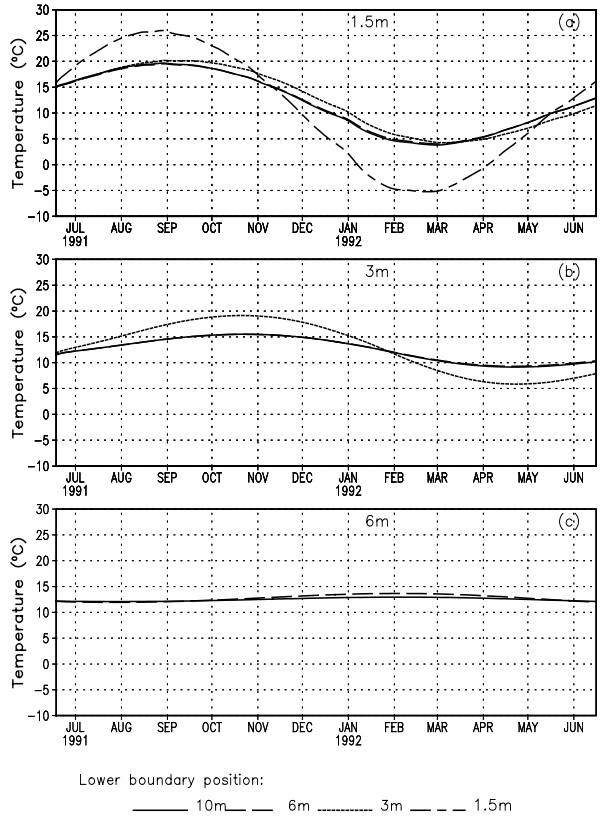

Fig. 3. Comparison of predicted daily mean temperature of the indicated depths with different lower boundary positions for HEIFE desert station.

ing Fig. 3c which displays the differences of two temperatures and the variation of their amplitudes at a depth of 6 m for the two lower boundary positions 6 m and 10 m deep, it can be found that both the difference and amplitudes reduce to very small values. From the figures, the explicit conclusion can be made that the lower boundary position has an important effect on both ground heat flux transport into the soil and the deep soil temperature profile, and a proper lower boundary position in this dry case should be located at a depth around 3 m to 6 m, which is approximately equal to the depth $3D$.

For the wet case test with the constant soil moisture wetness W ($W \equiv 0.75$), the heat conductivities estimated by J75 and MP81 are $k = 2.16$ W m^{-1} K^{-1} and 5.75 W m^{-1} K^{-1}, and the corresponding Ds are 2.8 m and 4.7 m. Figures 4 and 5 show the comparison of daily average temperature distributions at the different depths of 3 m, 6 m, 10 m and 15 m by using different lower boundary depths of 3 m (long and short dashed line), 6 m (dotted line), 10 m (dashed line) and 15 m (solid line) for the two schemes respectively. For the temperatures at a depth of 3 m shown in Figs. 4a and 5a, both the temperatures with boundary position 3 m deep are quite different from those with other boundary positions, the difference being about 10°C or more. The temperatures at a depth of 3 m with boundary positions 3 m deep also exhibit greater annual variation. The range of the variation is approximately from −5°C to 20°C for J75 and −10°C to 23°C for M81. For the other boundary depths of 6 m, 10 m, and 15 m, all the corresponding temperatures show smaller differences and the range of the differences are approximately equal to 2°C (for J75) and 4°C (for M81). All the temperatures bear a relatively small annual variation with amplitudes around 3°C to 15°C (for J75) and −2°C to 17°C (for M81). The feature of the temperature at depth 3 m for the wet case is quite similar to that at depth 1.5 m for the dry case mentioned above, except there is a depth shift. The other three sub-figures in Figs. 4 and 5 also present behaviors similar to those in the dry case but with a similar depth shift. Comparing Fig. 4 with Fig. 5, it can be found that, at the same depth, the amplitudes of the simulated temperatures using the MP81 scheme are greater than those using the J75 scheme. The reason is that the thermal conductivity (5.75 W m^{-1} K^{-1}) for the MP81 is much greater than that for J75 (2.16 W m^{-1} K^{-1}). Under the same moisture content conditions, the greater the thermal conductivity in the soil, the more heat transfer to the soil, and the deeper the damping depth of the diurnal and annual temperature wave for the soil. By further checking the temperature distribution at the depths of 3 m, 6 m, and 10 m and the temperature wave amplitudes at depths of 10 m and 15 m in Figs. 4 and 5, it is evident that the proper lower boundary positions are 6 m–10 m for J75 and 10 m–15 m for MP81. It also proves that the depth around $3D$ for the lower boundary position is a correct selection in the wet case. The features, that the temperature at the shallower depth predicted by the shallower lower boundary position (such as 1.5 m in the dry case in Fig. 3 and 3 m in the wet case in Figs. 4 and 5) exhibits greater annual variation amplitude than and more difference from those predicted by other deeper boundary positions, are ascribed to the significant influence of the boundary position on the heat transfer and storage in the soil body. When using zero flux as a boundary condition, the boundary actually acts as a heat barrier. It blocks the heat energy flow up or down across the boundary. Thus, the heat energy flux, which originally should flow down through the boundary in the warm season or go up through the boundary in the cold season, is blocked and so the energy accumulates up at the boundary. In turn, this will increase the temperature in the warm season and decrease the temperature in the cold season and enlar-

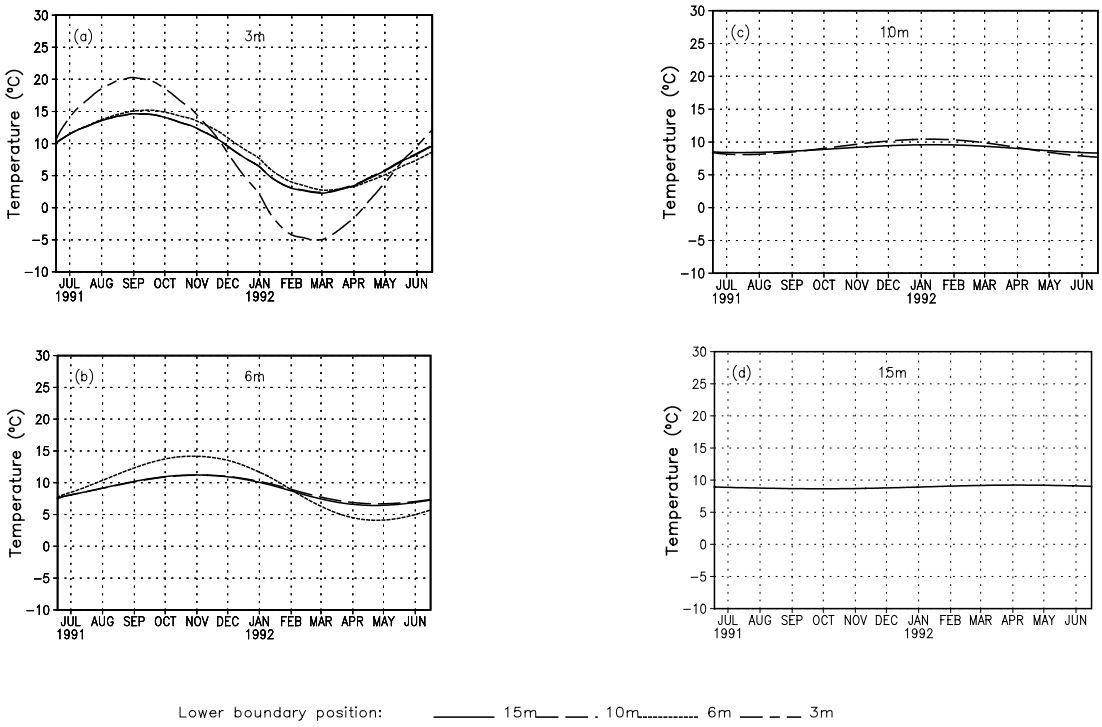

Fig. 4. Comparison of calculated daily mean temperatures at the indicated depth due to different lower boundary positions. Thermal conductivity scheme is J75 with constant wetness $W = 0.75$.

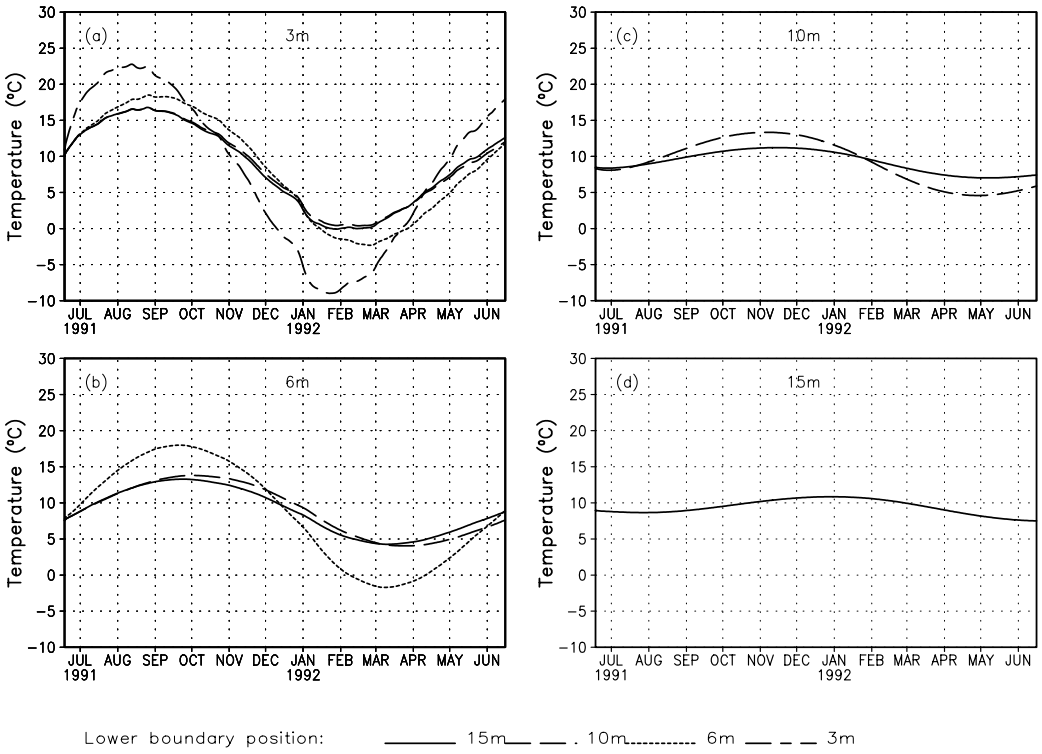

Fig. 5. As in Fig. 4 but for MP81.

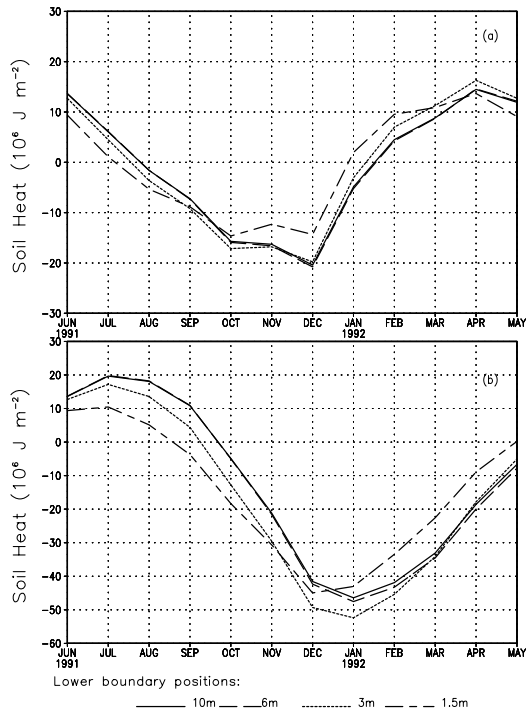

Fig. 6. Calculated values of (a) monthly and (b) cumulative variation of total energy stored by the soil body with different depths of the boundary position. The thermal conductivity scheme is NIU.

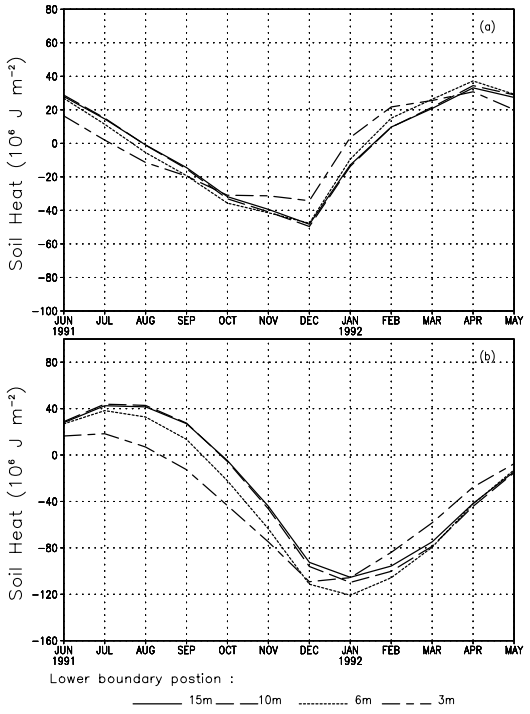

Fig. 7. As in Fig. 6 but with thermal conductivity scheme J75 with constant wetness $W = 0.75$.

ge the amplitude of the annual temperature wave at the boundary. The deviation of the predicted temperature from the real value depends on how much energy, which originally ought to be transported away from or into the boundary, is blocked and accumulated at the boundary. The more energy blocked, the greater the deviation of temperature produced.

In order to demonstrate the effect of the boundary position on the energy transport in the soil, the heat energy absorbed or released by the soil body in different seasons with different boundary positions are simulated. Figures 6, 7, and 8 present the results for both dry and wet soil cases. They depict the difference of heat energy absorbed or released each month and the cumulative variation of net gain of total heat energy stored from June to the current month by the soil body due to different boundary positions. Figure 6 presents the simulation results of the dry case for one year of HEIFE data, which corresponds to a small thermal conductivity k from the NIU scheme and a small damping depth. Figure 6a describes the heat energy absorbed (positive value) or released (negative value) each month, which is actually equal to the amount of the ground heat flux into or out of the soil surface in each month. There is an approximate 5×10^6 J m^{-2} difference of heat energy between the case with boundary position 1.5 m deep and the cases with boundary position 3 m, 6 m, and 10 m deep, while there is a smaller difference between the positions 3 m and 6 m (or 10 m) and little difference between the positions of 6 m and 10 m. This verifies the conclusion that the depth around 3–6 m ($\approx 3D$) is a correct position for the lower boundary. Figure 6b shows the cumulative variation of the total energy stored by the soil body with different depths of the boundary position, which indicates the heat capacity of the soil. Figures 7 and 8 show the results for wet soil, which are similar to the dry case. By comparing Fig. 7 with Fig. 8, the effects of the thermal conductivity on the correct boundary position setting are clearly revealed. The thermal conductivities from MP81 and J75 are 5.75 and 2.16 (W m^{-1} K^{-1}), respectively. The results from the figures show that the soil with greater thermal conductivity holds more heat capacity and in turn can absorb more heat energy in summer and then release it in winter. This makes the soil body more powerful in regulating the heat exchange between the air and the ground surface. Figures 7 and 8 also verify that the proper lower boundary positions are 6–10 m for the $D = 2.8$ m case and 10–15 m for the $D = 4.7$ m case (both are around 3 again!).

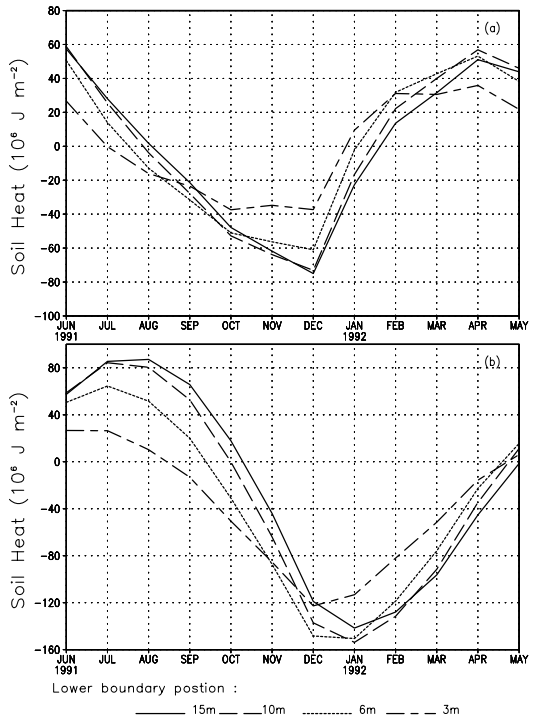

Fig. 8. As in Fig. 6 but with thermal conductivity scheme MP81 with constant wetness $W = 0.75$.

5. Conclusions and discussions

In this study, the effects of the lower boundary position setting on the heat balance of soil are reviewed. From the above discussion and reasoning, the following conclusions can be made. (1) The soil body as a heat carrier has its intrinsic heat capacity under annual heat wave forcing. The heat capacity is not allowed to be ill-natured, or otherwise the solution of the Fourier equation with a zero flux boundary condition will be distorted. (2) The volume of the heat capacity for a soil body is closely dependent on the annual wave damping depth, mainly determined by the thermal properties of the soil. (3) When using the Fourier equation with zero flux as the lower boundary condition, the selection of the lower boundary position should be made very carefully because an overshallow lower boundary position will limit the annual wave propagation downward into the entire soil zone, block up heat energy into or out of the soil zone and then misinterpret the intrinsic heat capacity owned by the soil zone. This will cause the energy balance in the soil to malfunction and in turn distort the energy exchange between the atmosphere and the ground surface. (4) In practice, it is impossible to locate lower boundary position at an infinitely deep depth. So, there should be a criterion for the position selection. According to the reasoning and numerical simulation results in this study, the depth of the position is very dependent on the annual wave damping depth. The proper depth for the lower boundary position may be three times the annual heat wave damping depth or more. For most soil textures, the proper lower boundary depth for the Fourier equation should be within a range of 6 m to 15 m, where the selection of the proper value mainly depends on soil properties and the soil moisture condition. Understanding the effect of the lower boundary position on the heat balance in the soil and the exchange between the ground surface and the atmosphere is important.

If the land surface is covered by both snow and vegetation, the annual soil temperature wave will propagate to a shallower depth than in bare soil because snow has a lower thermal conductivity and snow also acts as an isolator for the underlying soil. Since the overlap of snow, vegetation, and underlying soil varies in different seasons, it is better to select the lowest boundary position for different land surface cover for the whole year, which means to select the lower boundary position of bare soil. With regard to frozen soil with ice, the annual wave damping depth is much greater than unfrozen soil because the thermal conductivity of ice is 4 times that of water and the heat capacity of ice is one half of water. Accordingly, we should take a deeper lower boundary position in a frozen soil model.

Acknowledgments. The anthers would like to thank Prof. Xue Yongkang for critical and insightful review of this paper. This work was supported by the following projects of China: (1) National Natural Science Foundation of China under Grant Nos. 40233034 and 40075019, (2) KZCX2-SW-210, (3) National Natural Science Foundation of China under Grant No. 40305011.

REFERENCES

Avissar, R., and R. A. Piekle, 1989: A parameterization of heterogeneous land surface for atmospheric numerical models and its impact on regional meteorology. *Mon. Wea. Rev.*, **117**, 2113–2136.

Bonan, G. B., 1996: A land surface model (LSM version 1.0) for ecological, hydrological and atmospheric studies: Technical description and user's guide. NCAR Technical Note, NCAR/TN-417+STR. National Center for Atmospheric Research, Boulder, Colorado, 150pp.

Clapp, R. B., and G. M. Hornberger, 1978: Empirical equations for some soil hydraulic properties. *Water Resour. Res.*, **14**(4), 601–604.

Dai Yongjiu, and Zeng Qingcun, 1997: A land surface model (IAP94) for climate studies, Part 1: Formulation and validation in off-line experiments. *Adv. Atmos. Sci.*, **14**, 434–460.

Deardorff, J. W. 1978: Efficient prediction of ground surface temperature and moisture with inclusion of a layer of vegetation. *J. Geophys. Res.*, **83**, 1889–1903.

Gao Youxi, and Hu Yinqiao, 1994: *Advances in HEIFE Research* (1987–1994). Special Issue 1, China Meteorological Press. (in Chinese)

Gonzalez-Rouco, F, H. von Storch and E. Zorita, 2003: Deep soil temperature as proxy for surface air-temperature in a coupled model simulation of the last thousand years. *Geophys. Res. Lett.*, **30**(21), 2116, doi:10.1029/2003GL018264.

Lin, J. D., 1980: On the Force-restore method for prediction of ground surface temperature. *J. Geophys. Res.*, **85**(C6), 3251–3254.

Lynch-Stieglitz, M, 1994: The development and validation of a simple snow model for the GISS GCM. *J. Climate*, **7**, 1842–1855.

McCumber, M. C., and R. A. Pielke, 1981: Simulation of the effects of surface fluxes of heat and moisture in a mesoscale numerical model—Part 1: Soil layer. *J. Geophys. Res.*, **86**, 9929–9938.

Milly, P. C. D., 1982: Moisture and heat transfer in hysteretic, inhomogeneous porous media: A matric head-based formulation and a numerical model. *Water Resour. Res.*, **18**, 489–498.

Niu Guoyue, 1995: Numerical simulation and parameterization study on land surface process in dry and heterogeneous region. Ph. D. dissertation, Institute of Atmospheric Physics, Chinese Academy of Sciences, Beijing, China, 36pp. (in Chinese)

Peters-Lidard, C. D., E. Blackburn, X. Liang, and E. F. Wood, 1998: The effect of soil thermal conductivity parameterization on surface energy fluxes and temperature. *J. the Atmos. Sci.*, **55**, 1209–1224.

Philip, J. R., and D. A. de Vries, 1957: Moisture movement in porous material under temperature gradient. *Trans. Amer. Geophys. Union*, **38**, 222–228.

Retnakumari, K., G. Renuka, and G. Rao, 2000: Relation between pre-monsoon soil temperature and monsoon rainfall in a tropical station. *Mausam*, **51**, 365–66.

Rosema, A., 1975: A mathematical model for simulation of the thermal behavior of the bare soil, based on the heat and moisture transfer. Niwars-Publication No. 11, Niwars, 3 Kanaalweg, Delft, the Netherlands. 12–23.

Roesch. A., J .P. Schulz, and M. Wild, 1997: Comparison and sensitivity studies of the land-surface schemes in the ECHAM General Circulation Model and the Europa-Model. Report No. 244, Max-Planck-Instutute Fur Meteorologie.

Scanlon, B. R., and P. C. D. Milly, 1994: Water and heat fluxes in desert soils 2. Numerical simulation. *Water Resour. Res.*, **30**(3), 721–733.

Stieglitz, M. A. Ducharne, R. D. Koster, and M. J. Suarez, 2001: The impact of detailed snow physics on the simulation of snow cover and subsurface thermodynamics at Continental Scales. *Journal of Hydrometeorology*, **2**(3), 228–242.

Sun Shufen, 1987: Computation of moisture and temperature profiles in soils—The coupled model. *Acta Mechanica Sinica*, **3**(1), 44–51.

Sun Shufen, Zhang Xia, and Wei Guo An, 2003: A simplified version of the coupled heat and moisture transport model. *Global and Planetary Change*, **37**(3–4), 265–276.

Tang Maocang, and E. R. Reiter, 1986: The similarity between the maps of soil temperature in U. S. and precipitation anomaly of the subsequent season. *Plateau Meteorology*, **5**, 293–307. (in Chinese)

Thompson, S. L., and A. Pollard, 1995: A global climate model (GENESIS) with a land-surface transfer scheme (LSX). Part I: Present climate simulation. *J. Climate*, **8**, 732–761.

Verseghy, D. L., 1991: CLASS—A Canadian land surface scheme for GCMS. 1. Soil model. *International Journal of Climate*, **11**, 111–133.

Viterbo, P, and C. M. Beljaars, 1995: An improved surface parameterization scheme in the ECMWF model and its validation. *J. Climate*, **8**, 2716–2747.

Xue Yongkang, L. Yi, M. Ruml, and R. Vasic , 2002: Investigation of deep soil temperature- atmosphere interaction in North America. Presentation in Joint Session 6, Surface/Atmosphere interaction at 13th Symposium on Global Change and Climate Variation.

Wang Wanqiu, 1991: Numerical simulation of the impact of soil temperature/wetness on short-term climate change. *Chinese J. Atmos. Sci.*, **15**, 115–123. (in Chinese)